

Effective Static Response Compensation Suitable for Low-Power ASIC Implementation with an Application to Pressure Sensors

Christophe Berthoud, Michael Ansorge, and Fausto Pellandini

Institute of Microtechnology, University of Neuchâtel

Rue Breguet 2, CH-2000 Neuchâtel, Switzerland

Phone: +41 32 718-3200 Fax: +41 32 718-3201 E-mail: berthoud@imt.unine.ch WWW: <http://www-imt.unine.ch>

Abstract - This paper presents an efficient all-digital compensation technique for sensors measuring static or slowly-varying quantities such as pressure. The proposed solution compensates the temperature dependencies and further non-linearities affecting the accuracy and measurement range of the sensors. In addition, for the considered pressure sensors, the trimming that is usually performed in factory can be replaced by a measure of the sensor characteristics to be used for the digital sensor compensation. The whole design procedure, starting from the description of the pressure sensors down to the low-power ASIC implementation of the processor architecture is discussed in detail.

I. INTRODUCTION

With the advent of modern microtechnologies and their impact on the field of sensors, in particular with regard to performance improvement, increased miniaturization level, and cost reduction, solid-state sensors are becoming largely used. The application potentialities, especially in the domains of portable instrumentation, and microsystems, are very extended.

The present paper proposes a contribution for an all-digital compensation of sensors measuring static or very slowly-varying quantities such as pressure, including barometric and altimetry measurements, or laminar flow measurement.

The response of these sensors is usually affected by various phenomena such as hysteresis, temperature dependency, and non-linearities, where the last effects can in turn be subdivided into the contribution of non-linear terms (1) in the temperature performance, and (2) in the performance of the measured quantity (e.g. pressure). Basically, these effects are under the control of the manufacturers by selecting appropriate device structures and technological processes. Furthermore, each sensor device can be calibrated individually and compensated by means of on-chip trimming facilities to achieve the specified accuracy and measurement range. To completely suppress the trimming of the sensors in order to cut manufacturing costs, specially in case of laser-trimming, there is a clear motivation to use an electronic compensation of the sensors, a solution which provides in the same time an improvement of the overall accuracy and an extension of the measurement range.

This paper presents an efficient all-digital compensation technique handling both temperature dependencies and non-linearities. A compact fixed-point processor architecture was designed for a low-power VLSI implementation. The core of the architecture consists of a polynomial processing unit that is embedded in an iterative root-solving algorithm used for the extraction of the compensated signal value.

As an example, the concept was applied to real pressure sensors available on the market. The performance achieved shows that for the considered sensors, it is possible to suppress the trimming of the devices while enhancing the overall accuracy. Alternatively, the measurement range can also be enlarged.

The paper is outlined as follows. First, Chapter II presents the principles and the modeling of the considered pressure sensors whereas Chapter III introduces the proposed compensation method. The sensor system with the compensation unit is then discussed in Chapter IV. The digital compensation circuit is presented in Chapter V, including simulation results. Next, the hardware implementation aspects are covered in Chapter VI. Finally, Chapter VII concludes the paper.

II. SENSOR MODELING

The sensor modeling is applied to piezoresistive pressure sensors that are silicon integrated systems containing a Wheatstone bridge with piezo-resistances implanted on a thin diaphragm. The pressure is measured on the differential output of the bridge. The main problem with these sensors is their temperature dependency and the mismatch of the bridge resistances. Both affect in an important way the accuracy of the measurement unit and limit the range of use of the sensors.

1) Behavior modeling : We propose to establish a model of the pressure behavior for the sensor response. This model is based on a bivariate second-order polynomial model (1). P_{meas} corresponds to the measured quantity as provided by the non-ideal physical pressure sensitive device and P_{ext} is considered as the external value. As the measure of the pressure is disturbed by the

temperature, the model (1) contains the expression of the external temperature T_{ext} . A second-order polynomial model (2) is used to interpolate the measured temperature T_{meas} .

$$P_{meas} = \sum_{j=0}^2 \left[\sum_{k=0}^2 b_{jk} T_{ext}^k \right] P_{ext}^j = \sum_{j=0}^2 c_j P_{ext}^j \quad (1)$$

$$T_{ext} = \sum_{j=0}^2 a_j T_{meas}^j \quad (2)$$

Fig. 1 shows the pressure sensor with these two measured quantities.

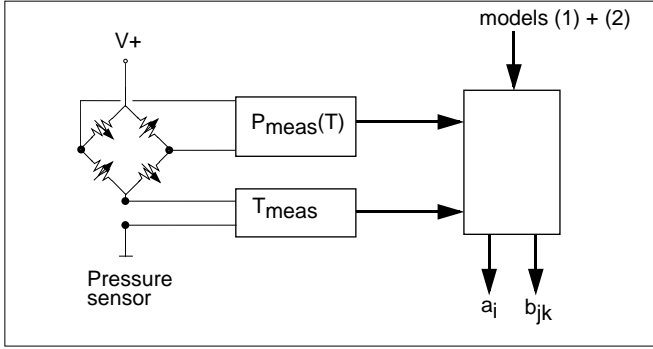


Fig. 1. Behavioral model of the sensor's response.

2) Model parameters : The determination of the model parameters b_{jk} (1) is executed by measuring P_{meas} at five different pressures and five different temperatures, twenty-five points at all. First, root-mean-square (RMS) interpolations of the measured pressure points are determined for each temperature. With these values, we evaluate RMS interpolations in temperature. Also we obtain the nine coefficients b_{jk} which characterize the quadratic interpolation surface of the measured points. Once those parameters are known, the three coefficients c_j (1) can be evaluated at any temperature of the range. This way the theoretical offset, the sensitivity and the slope variation of the sensitivity can be computed for the external temperature condition. We determine the model parameters a_j (2) by calculating the RMS interpolation of the measured temperature points. The temperature is measured over the bridges resistances. This parameters are called temperature coefficient resistors TCR 0, 1, 2.

III. COMPENSATION METHOD

Once we have defined a model of the behavior of the sensor we use a compensation method to correct the measured values (Fig. 2).

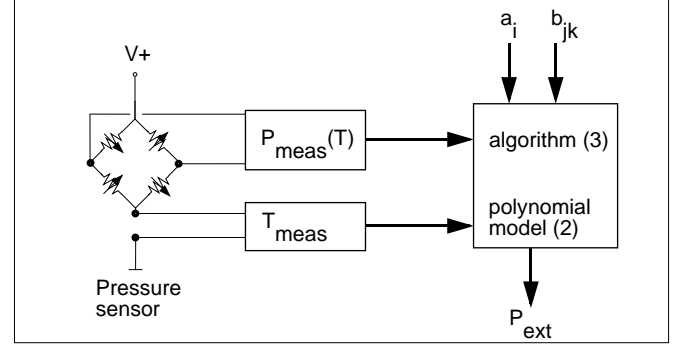


Fig. 2. Use of the model for compensation

1) Compensation method : Our compensation method using digital circuitry works as follows: First, we solve (2) for T_{ext} by computing the polynomial model of the external temperature. As soon as we have extracted this information the three parameters c_j (1) are determined. Then, P_{ext} is compensated using the iterative algorithm (3) rather than the classical second-order equation solving method. Through the use of this algorithm, square roots and divisions can be avoided, an important advantage when an implementation in digital hardware is aimed.

$$P_{ext}(i+1) = P_{ext}(i) + \left[P_{meas} - \sum_{j=0}^2 c_j P_{ext}^j(i) \right] \quad (3)$$

$$\text{for } i = 0, 1, 2, \dots; \text{ with } P_{ext}(0) = P_{meas}$$

That way, we get the external pressure according to the model. The number of iterations depends on the desired accuracy. Overall convergence conditions of the iterative algorithm can be found in [1].

2) Numerical example : The benefits of the method are illustrated in the following example. We have chosen an absolute pressure sensor specified for a nominal full-scale pressure of 1 (bar) [2]. The sensor is supplied by a constant voltage source. Table 1 shows an example of the maximum errors among five pressure measurements in percent of full scale (% F.S., 1 (bar)) between the external pressure and two interpretations of the sensor measure at different temperatures. The first column corresponds to a direct mapping of the measured pressure from a non laser-trimmed sensor at a reference of 0.5 (bar) and 25 (°C). The second column corresponds to the results after two iterations with our compensation method.

TABLE I
MAXIMUM ABSOLUTE ERRORS (% F.S.): EXTERNAL PRESSURE VS. PROCESSED VALUE FOR FIVE TEMPERATURES AND FOR TWO INTERPRETATIONS OF THE SENSOR MEASURE.

Error of various sensor signals after conversion in (bar)	Maximum Abs. Error % F.S. direct measured output	Maximum Abs. Error % F.S. compensated signals, two iterations

-40°C	18.1	0.64
0°C	8.4	0.13
25°C	2.9	0.08
75°C	7.0	0.24
120°C	15.7	0.32

The table shows the efficiency of the compensation algorithm. The overall accuracy of a piezoresistive pressure sensor is enhanced, in particular concerning the temperature compensation. Furthermore, the usable range of pressure measurement can be enlarged in an important way since the second-order polynomial model of the sensor's behavior takes into account the loss of sensitivity of the pressure-sensing device.

IV. SENSOR AND COMPENSATION SYSTEM

A full digital compensation system has been developed to correct both the temperature and the pressure measured by the sensor. Fig. 3 shows the parts of the measure path.

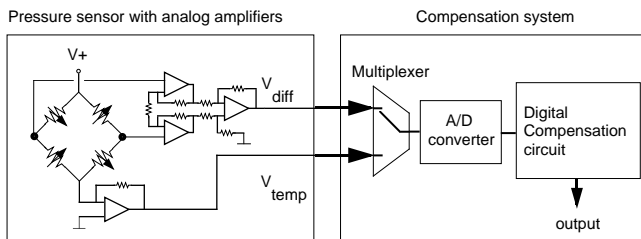


Fig. 3. Principle of digital compensation applied to a piezoresistive pressure sensor.

The sensor is composed of the pressure sensitive device and the analog amplifiers. In the analog part there is one differential amplifier for the pressure output V_{diff} and one current-to-voltage amplifier for the measure of the temperature V_{temp} . As the sensor is supplied by a constant voltage and since the resistance of the whole bridge changes with temperature, the measure of the current trough the bridge is a possible way to determine the external temperature.

Next, the A/D converter quantifies the measured voltage values. Finally, the digital compensation circuit treats the information to enhance the overall accuracy of the measurement system.

One advantage of this full-digital compensation is that the correction can also take into account the non-linearities and the temperature effects of the analog electronic (amplifiers) and the mixed (A/D converter) parts as well. This is only possible if the modeling has been performed trough these elements.

The next chapter discusses in detail the architecture of the low-power ASIC for the compensation circuit we have developed.

V. DIGITAL COMPENSATION CIRCUIT

The compensation method developed has been realized on a specific architecture. The goal of this implementation is three-fold: (i)

to outperform the classical laser-trimming method, (ii) to keep the costs as low as possible, and (iii) to minimize circuit area and power consumption such that the device can also be used in battery-powered systems. The main blocks of the digital compensation unit developed are shown in Fig. 4.

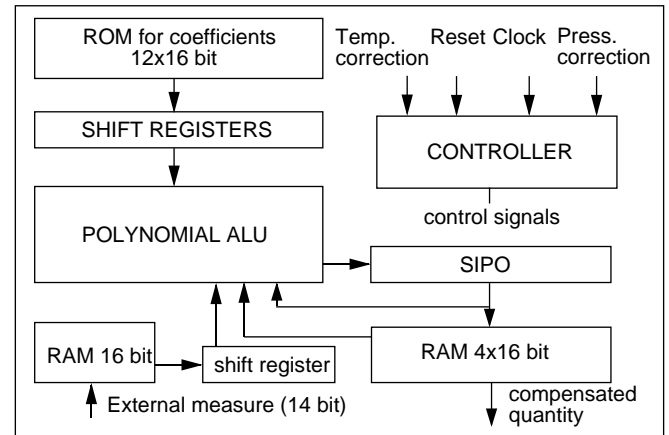


Fig. 4. Architecture of the compensation circuit in test configuration: 14-bit ADC and 16-bit representation for coefficients, partial results and output

1) Polynomial ALU : The polynomial arithmetic logic unit (PALU) forms the core of the architecture, treating two's-complement, fixed-point numbers. The core of this ALU is derived from [3], [4] and optimized for low-power consumption (Fig. 5).

$$P = \sum_{i=0}^n a_i x^i = (((a_n x + a_{n-1})x + a_{n-2}) \dots)x + a_0 \quad (4)$$

Obviously, the PALU is based on Horner's scheme (4). Accordingly, it is subdivided into elementary units handling monomials. A polynomial is then processed either by time-multiplexing a single monomial block, or by cascading as many instances as required by the degree of the polynomial.

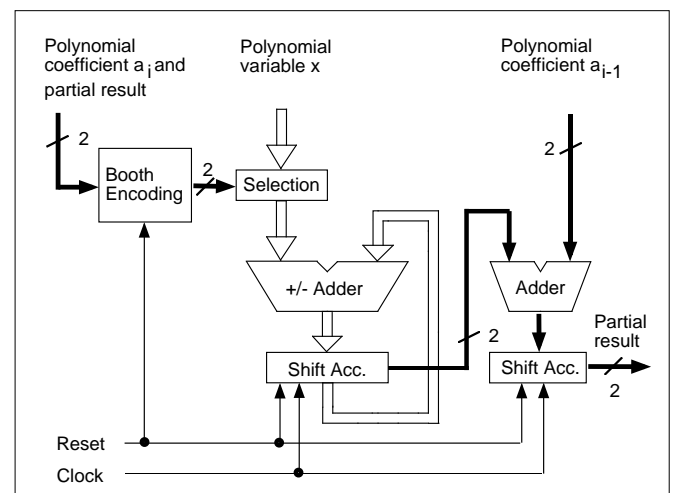


Fig. 5. Scheme of a monomial block.

Each monomial block is structured as follows :

- The multiplication is realized using a modified Booth encoder [3].
 - The architecture of the ALU is bit parallel-serial, the variable of the polynomial is processed in parallel, while the coefficients and the partial results are processed serially. This scheme results from the selected Booth encoder, handling two bits at a time.
 - Product and addition are processed serially, such that carry propagation occurs only on one bit per cycle.
 - The numbers are represented in two's complement form.
 - $(m \cdot n)/2 + 3$ cycles are necessary to evaluate a monomial, where n is the wordlength of a_i and m the wordlength of the variable x .
- Using this architecture, we get an interesting time/surface ratio for the polynomial evaluation (see chapter VI for hardware implementation).

2) Bit-true simulation : To validate the digital compensation approach and to decide on the wordlength needed to code the coefficients, a bit-true simulation with Matlab™ has been done. The simulation results show that a 14-bit A/D converter for both temperature and pressure measures is required such that the digital noise does not influence the final accuracy to be achieved. Coefficients and partial results are represented with 16-bits.

Fig. 6 shows the error in percent of the full scale between the polynomial model of the sensor's response and the external pressure at a fixed temperature of 25° (C), then after one iteration of the compensation algorithm (3) based on the polynomial model and finally after two iterations.

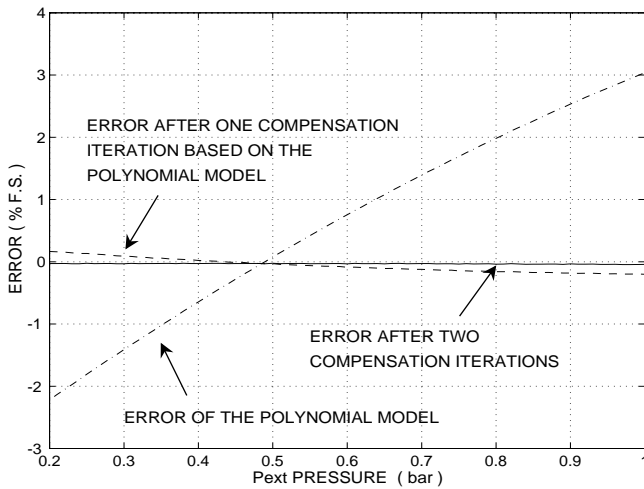


Fig. 6. Error (% F.S.) between the polynomial model before and after compensation and the external pressure for the full pressure range (25° (C)).

One typical response characteristic for such sensors – the non-linearity – is also influenced by the temperature. Table II shows this non-linearity at five temperatures before and after compensation.

TABLE II

NON-LINEARITY ERROR (% F.S.) WITH RESPECT TO THE BEST STRAIGHT LINE.

Temp. (°C)	-40°	0°	25°	75°	120°
Error without compensation in % of F.S.	0.3639	0.2946	0.2514	0.1673	0.0969
Error with compensation in % of F.S.	0.0968	0.0229	0.0076	0.0030	0.0015

The achieved residual non-linearity outperforms the one of the laser-trimmed sensors ($\pm 0.05\%$ F.S. at 25 °C) [2] by a factor greater than 6.

Fig. 6 and Table II illustrate well how effective this digital compensation method is to correct (i) the temperature dependencies of piezoresistive pressure sensors and (ii) to increase the overall accuracy. Furthermore, this increased accuracy can be used to extend the usable measurement range.

VI. HARDWARE IMPLEMENTATION

The hardware implementation has been done according to a modern top-down design methodology using VHDL and a logic synthesis tool. A monomial block has been realized in full-custom design allowing for a precise indication on area and power consumption for this key element. Furthermore, a rough estimation for the overall chip became possible.

1) VHDL model specification and simulation: With the processing unit's architecture globally specified, the design has been captured with the modeling and simulation tool SpeedCHART™ [5]. Once the signals of the internal control circuit defined, the design has been thoroughly tested by simulation. Table III summarizes the computation time expressed in clock periods, first for the temperature determination and then for the pressure compensation for different steps. Obviously, the number of iterations determines the accuracy of the compensated output.

TABLE III
CLOCK PERIODS VS. OUTPUT ACCURACY

	Temp. determination	Sensor Parameter	Pressure compensation (# iterations)		
			0	1	2
Text (°C) 75	76.68				
Pext (bar) 0.7			0.7139	0.6988	0.6997
periods	+ 118	+ 362		+ 134	+ 134
total # of periods	118	480		614	748

Taking into consideration a maximum of 1 kHz for the bandwidth of a typical pressure sensor, the clock frequency would remain near to 1 MHz, a reasonable value even for low-power technologies.

2) Logic synthesis: The SpeedCHART™ circuit model has than been translated into VHDL and fed into a logic synthesizer, configured for the 1.2 micron technology CSEL_LIB of CSEM (Centre Suisse d'Electronique et de Microtechnique, Neuchâtel, Switzerland). The final layout processed with COMPASS' layout tools can be characterized with the following figures (Table IV).

TABLE IV

LOGIC SYNTHESIS IMPLEMENTATION OF THE TEST CONFIGURATION

# standard cells	2114
# transistors	25373
circuits area	5.16 mm ²

Obviously, a better result could be achieved with full-custom design (see below) and more evolved logic synthesis tools. Nevertheless, the VHDL description has the important advantage to be very easily portable among different technologies but also on FPGAs for rapid prototyping.

3) Full-Custom design: In order to figure out both the economy in surface and power that could be achieved through a full-custom design, a key element – the monomial ALU – has been hand-designed for the same technology on COMPASS' layout tool (Fig. 7).

The key numbers for the ALU are shown in table V, the values for the complete circuit have been estimated according to the experiences made with the ALU as well as based on previous experiences [6].



Fig. 7. Layout of the monomial block designed to perform polynomial evaluation ($395 \cdot 1140 \lambda^2$).

TABLE V

FULL-CUSTOM IMPLEMENTATION OF THE TEST CONFIGURATION

	monomial ALU	test configuration (estimated)
# transistors	1216	11700

circuit area	0.16 mm ²	2.4 mm ²
energy consumption ¹	0.29 nJ per multiplication/addition	N/A

¹ power supply 2V, master clock 3.125 MHz

VII. CONCLUSION

In this paper, we presented an all-digital circuit for the compensation of temperature dependencies and non-linearities of sensors.

First, a sensor model has been established, using a second-order polynomial model for the measured temperature of the bridge and a bivariate second-order polynomial model for the main quantity measured. Then, the temperature is determined. Based on this result, the coefficients of the second model are computed, and finally the equations for the main quantity solved.

For our application – a piezoresistive pressure sensor – the results are convincing. After the evaluation of the temperature and 2 iterations of the compensation algorithm for the pressure, we got a full scale error for the non-linearity from 0.0076 % F.S. at 25° (C), a result approximately 6 times better than with conventional laser-trimmed sensors.

This compensation method could be applied not only to pressure sensors, but to many other low-frequency measurement systems which are suffering from the same problems: temperature dependencies and non-linearities.

The realization of a dedicated polynomial ALU and the use of an iterative algorithm enable us – due to the low-area and low-power hardware – to conceive smart sensors for portable applications. Furthermore, it can be adapted easily to a digital communication interface, e.g., an I²C, enabling hence for use in more complex and distributed data acquisition and control systems.

In a future step, the joint implementation of sensor, converters and compensation electronics on a single device will be studied: a monolithic full-digital smart pressure sensor seems possible in a near future.

ACKNOWLEDGMENT

The authors are grateful to Mr Daniel Otter from Micronas Semiconductor S.A. and to Marc Boillat for the stimulating discussions on solid-state pressure sensors. The authors express also their gratitude to Alexandre Heubi for the provided concepts, and his guidance during the hardware implementation. Finally, the contribution of Hans Peter Amann for the preparation of the final paper was greatly appreciated.

This work was supported by the Swiss National Found for Scientific Research under Grant FN 94 2000 - 40627.94.

REFERENCES

- [1] C.E. Fröberg, "Introduction to Numerical Analysis", 2nd Ed., Addison-Wesley, Reading, MA, USA, 1969, (1979, 5th printing), pp. 33-39.
- [2] Am5801AV.048, data sheet, Micronas Semiconductor S.A., 2022 Bevaix, Switzerland.
- [3] A. Heubi, S. Grassi, M. Ansorge, and F. Pellandini, "A Low Power VLSI Architecture for Digital Signal Processing with an application to Adaptive Algorithms for Digital Hearing Aids", Proc. EUSIPCO'94, Edinburgh, Scotland, UK, Sept. 1994, pp. 1875-1878.
- [4] J.-M. Muller, "Arithmétique des ordinateurs, opérateurs et fonctions élémentaires", Masson, Paris, F, 1989, pp. 108-114.
- [5] K. Bettaieb, T. Brückner, "SPeeDCHART : a New Way to Design ASICs", Proc. ASIC'93, Nürnberg, FRG, June 1993
- [6] D. Sun, H. P. Amann, A. Heubi, F. Pellandini, "Design Automation in Digital Signal Processing : synthesizable VHDL models for rapid prototyping", Proc. GRETSI'95, Juan-Les-Pins, France, Sept. 18-21, 1995, pp. 1065-1068.